

Audio-Frequency Current Comparator Power Bridge: Development and Design Considerations

NILE M. OLDHAM, MEMBER, IEEE, O. PETERSONS, FELLOW, IEEE, AND B. C. WALTRIP

Abstract—The development, design, construction, and partial evaluation of a system for performing active and reactive power measurement from 50 to 20 kHz is described. The technique is an extension of a power bridge based on a current comparator capacitance bridge that was originally restricted to power frequencies. The design features and component characteristics for wide-band operation are emphasized. A digitally synthesized, dual-channel signal source provides the required voltage and current signals.

I. INTRODUCTION

ACTIVE AND reactive power measurements at frequencies above the normal frequency range of 50–400 Hz are becoming more commonplace in equipment where weight and efficiency are of prime concern. Standards to support audio-frequency wattmeters exist in the form of dual-channel digital sampling instruments [1]. While sampling techniques are very powerful (particularly when measuring highly distorted waveforms), uncertainties smaller than ± 0.1 percent (± 1000 ppm) are difficult to achieve over the audio range. At power frequencies, uncertainties of ± 15 ppm are achieved using impedance bridge techniques which ultimately rely on thermal voltage converters to relate the ac voltage to a dc voltage standard, and an accurately known ac resistance [2], [3]. The system described in this paper extends this technique to 20 kHz while maintaining measurement uncertainties under ± 200 ppm of apparent power.

II. MEASUREMENT SYSTEM

A. Operating Principles

A block diagram of the audio-frequency power bridge is shown in Fig. 1. As in a previous system [2], the wattmeter under test (MUT) is supplied by a dual-channel digital waveform generator followed by power amplifiers A_V (voltage) and A_I (current). The test voltage is scaled from 120 or 240 V to 10 V with a two-stage transformer. Two such transformers are required to cover the audio-frequency range—one for frequencies between 50 Hz and 1 kHz and the other for frequencies between 1 and 20 kHz. The test voltage is determined by measuring the low-level output of one of these transformers using a thermal ac-dc voltage comparator (TVC). Reference currents I_1 and I_2

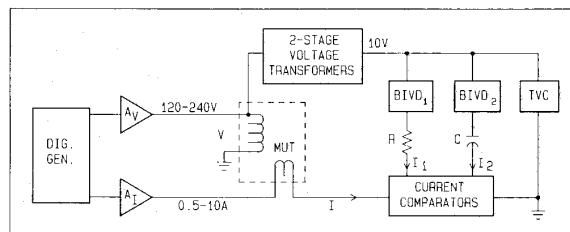


Fig. 1. Block diagram of the audio frequency power bridge.

are established with wide band, active binary-inductive-voltage dividers (BIVD's) and impedances R and C . The center-tapped symmetry of the BIVD's provides excellent frequency response [4] and thus only one divider for each impedance (R and C) is needed to cover the audio range. The test current I (0.5–10 A) is compared with the sum of I_1 and I_2 (1 mA) in one of two specially designed current comparators which are required to span the audio-frequency range. The crossover point between the low and high frequency comparators is also about 1 kHz. At balance the active power, P , applied to the wattmeter under test (MUT), may be expressed in terms of

$$P = kV^2/R$$

where

- V the applied voltage,
- R the resistance connected between BIVD₁ and the current comparator (Fig. 1),
- k a constant involving the current comparator, voltage transformer, and BIVD ratios.

B. Digitally Synthesized Source

The signal source is a digital waveform generator [5] which synthesizes two low-level sinusoidal signals at frequencies between 50 Hz and 20 kHz. In this technique the waveforms are constructed by sequentially applying up to 2048 values stored in read/write memory to a pair of multiplying digital-to-analog converters (MDAC's) which produce voltage waveforms with peak amplitudes between 0–10 V. The amplitudes are independently adjustable by controlling the dc references of each MDAC. The phase relationship of the two signals is adjusted by changing the set of values stored in one of the memories. These signals are applied to high-voltage amplifier A_V [6] and

Manuscript received June 10, 1988.
The authors are with the Electrosystems Division, National Bureau of Standards, Gaithersburg, MD.
IEEE Log Number 8825618.

transconductance amplifier A_1 [7], which then supply synthetic power to the MUT.

The voltage and current are programmable between 0–280 V and 0–7 A, respectively, with a precision of 4 ppm of full scale. The phase angle between the voltage and current waveforms may be adjusted with a precision of 1–100 μ rad, depending on the frequency. The short-term stability of the power applied to the MUT is typically ± 10 ppm. This is further enhanced by a servo-loop (described later), which slaves the test current to the test voltage.

C. Voltage Circuit

Referring to the detailed circuit diagram shown in Fig. 2, a two-stage, voltage transformer T_1 is used to scale the test voltage V to V_1 (nominally 10 V). This voltage is measured by comparing it to a 10-V dc reference using a thermal ac–dc voltage comparator similar to the one described in [8]. The magnitude and phase of the test voltage is computed based on this measurement and a knowledge of the transformer in-phase and quadrature errors.

Both the BIVD's and the TVC present substantial loads to the transformer and the technique for minimizing loading errors is shown in Fig. 2. The BIVD's are constructed as two-stage dividers and, thus their magnetizing currents may be supplied from a separate set of windings (N_4) on the main core of T_1 . This induces the approximate operating voltage across the BIVD ratio winding and effectively increases its input impedance by a factor 1000 or more (depending on the first-stage errors of the transformer and divider).

A similar technique involving an operational amplifier is used to increase the effective input resistance, R_T , of the TVC. Amplifier A_1 , with a gain of two, produces a 20-V signal which is connected to the TVC through resistor R_{T1} . If R_{T1} is approximately equal to R_T , A_1 will supply most of the TVC input current. The ratio winding, N_3 , of the transformer must supply only the error current required to maintain the precise 10-V level at the TVC. Thus the effective input resistance to the TVC may be increased by a factor of 1000 or more (depending on the gain of A_1 and the ratio R_T/R_{T1}). This "current pump" circuit is very effective at power frequencies where the amplifier can precisely double its input voltage; however, at higher frequencies performance is degraded somewhat by amplifier phase errors.

As mentioned, two voltage transformers are required to span the 50 Hz–20 kHz frequency range. The low-frequency transformer, designed to operate between 50 Hz–1 kHz was constructed using a large magnetizing core with 1200 primary turns (N_1). The BIVD drive winding N_4 consists of 100 turns tapped for different voltages. The primary ratio winding N_2 (also 1200 turns) and the secondary ratio winding N_3 (100 turns) are wound around both the magnetizing and ratio cores (see Fig. 2). The high frequency transformer, designed to operate between 1–20 kHz, is constructed with smaller cores and fewer windings to minimize interwinding capacitance. The

maximum in-phase and quadrature errors of these transformers are given in Table I (see Section III).

The reference currents I_1 and I_2 are generated by scaling the voltages applied to R and C using 24-bit, two-stage binary inductive voltage dividers. Three 8-bit sections are cascaded to provide 24-bit precision, and the first two sections are coupled using two-stage techniques to minimize loading effects. As in the voltage transformers described above, an extra winding on the magnetizing core is used to drive the following stage. Each section consists of 8 center-tapped windings in a binary sequence (256, 128, 64, \dots , 2 turns) which are interconnected using relays [9].

Because the impedances used to generate I_1 and I_2 are small compared to the output impedance of the BIVD's, the "current pump" circuits shown in Fig. 2 must be employed. Similar to the circuit used with the TVC, amplifiers A_2 and A_3 provide most of the load current and the BIVD's must supply only the small current required to correct the voltage developed at the terminals of R and C .

Each binary section consists of a twisted pair connected in series to provide the center tap. This technique leads to fairly large interwinding capacitance; however, because of the symmetry of the windings, the center tap is extremely accurate over a wide frequency range and a single BIVD operates over the entire power and audio range. The maximum in-phase and quadrature errors (based on comparisons with decade divider standards) are given in Table I.

D. Current Circuit

Reference current I_1 (0–1 mA) is defined by $V_1 d_1/R$, where d_1 is the ratio of BIVD₁ and R is a 4-terminal, 10-k Ω metal-film resistor. The maximum in-phase and quadrature errors of this resistor (based on comparisons with calibrated film resistors and standard capacitors) are given in Table I.

Reference current I_2 (also 0–1 mA) is defined by: $V_1 d_2 j\omega C$, where d_2 is the ratio setting of BIVD₂ and C is one of four three-terminal capacitors needed to cover the frequency range 50 Hz–20 kHz. At the higher frequencies gas capacitors may be used to produce the desired reference current. These capacitors have very low losses and small temperature coefficients. At lower frequencies where larger value capacitors are needed to produce the required current, polystyrene-dielectric capacitors were selected. These capacitors have relatively low losses (dissipation factors of 50–100 ppm compared to 10 or less for gas dielectrics), which are quite stable with temperature and time.

For active power, only the dissipation factor must be known accurately since loss current in I_2 adds directly to the in-phase current I_1 . For reactive power, the capacitance also must be known and the temperature coefficient of capacitance for the polystyrene units is approximately 100 ppm/ $^{\circ}$ C. This limits the accuracy of reactive power measurements made using this bridge. Capacitor calibra-

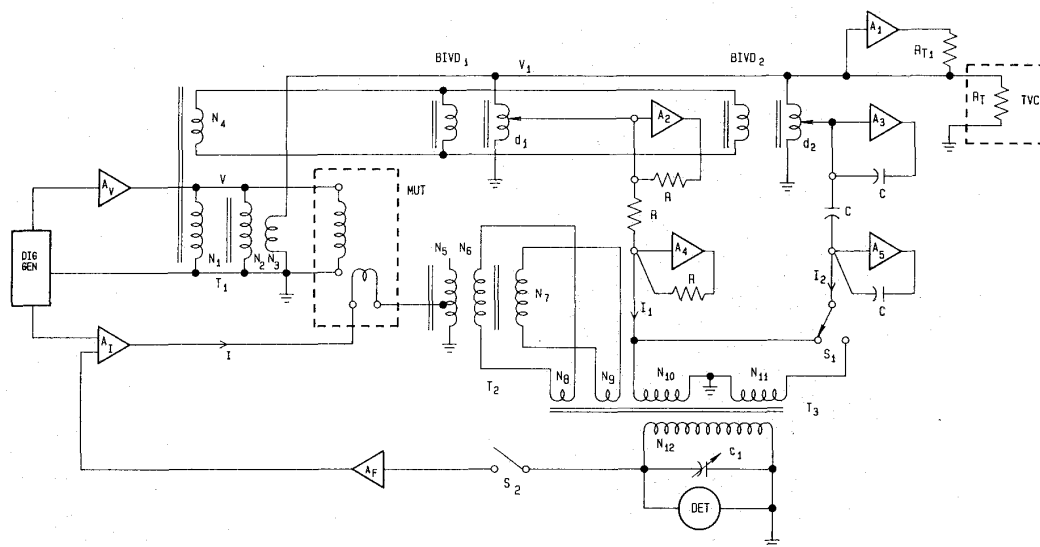


Fig. 2. Detailed system diagram of the audio frequency power bridge.

TABLE I
ESTIMATED UNCERTAINTIES IN PARTS PER MILLION OF APPARENT POWER

Parameter	50-60 Hz	>60 Hz - 1 kHz	>1 - 20 kHz
V_1 (TVC)	$\alpha = 5$	$\alpha = 10$	$\alpha = 30$
T_1 (V Transformer)	$\alpha_1 = 2$	$\beta_1 = 2$	$\alpha_1 = 5$
d_1 (BIVD ₁)	$\alpha_2 = 2$	$\beta_2 = 2$	$\alpha_2 = 5$
d_2 (BIVD ₂)	$\alpha_3 = 2$	$\beta_3 = 2$	$\alpha_3 = 5$
R	$\alpha_4 = 2$	$\beta_4 = 10$	$\alpha_4 = 3$
C	$\alpha_5 = 50$	$\beta_5 = 10$	$\alpha_5 = 100$
T_2 (I Transformer)	$\alpha_6 = 3$	$\beta_6 = 3$	$\alpha_6 = 10$
T_3 (I Comparator)	$\alpha_7 = 2$	$\beta_7 = 2$	$\alpha_7 = 3$
ω (Frequency)	$\alpha_8 = 1$	$\beta_8 = 1$	$\alpha_8 = 1$
U_D (coefficients)	A=11	B=11	A=23
U_Q (coefficients)	C=51	D=11	B=23

tions at the required accuracy level are not available routinely at NBS. Thus a scheme is being developed for intercomparing all four capacitors to a well-characterized 1-nF gas-dielectric capacitor. The uncertainty of measurements to date (for both capacitance and dissipation factor) are given in Table I.

The test current I , is scaled to 100 mA in a two-stage current transformer, T_2 . The primary winding, N_5 , is 20 turns tapped for 0.5-, 1-, 2.5-, 5-, and 10-A input currents. The 100-turn secondary and tertiary windings (N_6 and N_7) provide the 100-mA secondary and error currents to T_3 . A current transformer of similar design has been shown to have in-phase and quadrature errors of less than 15 ppm from 50 Hz–10 kHz. Estimates of the in-phase and quadrature errors over the full frequency range are given in Table I.

This scaled-down version of test current is compared to the reference currents, I_1 and I_2 in current comparator T_3 . Nominally, the 100-mA current in the one-turn winding N_8 (N_9 carries only a small error current) is balanced against the 1-mA reference current in 100-turn windings N_{10} and/or N_{11} . At unity power factor with $I_1 = 1$ mA and $I_2 = 0$, the current comparator will balance if the test current is in phase with the test voltage and has the appro-

priate magnitude to produce 100 mA in N_8 . At zero power factor with $I_1 = 0$ and $I_2 = 1$ mA, balance is obtained when I_2 is connected to N_{10} (using switch S_1) and the current leads the voltage by 90° , or when I_2 is connected to N_{11} and the current lags the voltage by 90° . At other power factors a combination of I_1 and I_2 produces a 1-mA current with the appropriate phase angle to balance the test current. Balance is achieved by adjusting I , I_1 , and I_2 to null the detector connected across the detection winding N_{12} . The variable capacitor C_1 is used to tune N_{12} for resonance. Balance may be done manually, remotely under computer control, or automatically by closing switch S_2 which drives the voltage across N_{12} to zero by amplifying the imbalance signal in A_F and feeding it back through the transconductance amplifier A_T . The latter effectively forces I to track V , thus eliminating any instability in the current channel.

To maintain low input impedances of the windings N_{10} and N_{11} and to minimize their interwinding capacitances, the number of turns was limited to 100 in each winding. Assuming a nominal value of 1 mA for I_1 , 1-ppm resolution requires the detection of 1- or 100-nA turns. Sensitivity depends on the number of turns in the detection winding, N_{12} , the permeability and dimensions of the core, and the operating frequency. An obvious means for increasing the sensitivity is to increase the number of turns in the detection winding. However, this reduces the frequency range by lowering the self-resonant frequency due to the increased interwinding capacitance.

In view of the above considerations, two current comparators were selected with a crossover frequency at 1 kHz. The low-frequency unit has a toroidal core with 1100 turns in the detection winding while the high-frequency unit has a smaller core with 200 detection winding turns. Both current comparators have magnetically shielded sensing cores and two-stage (compensated current com-

parator-type) construction as described in [10]. The measured in-phase and quadrature errors are given in Table I.

Additional current pumps are needed to ensure that the currents in N_{10} and N_{11} are strictly a function of the BIVD output voltages and the impedances R and C . Amplifiers A_4 and A_5 supply the current for lead and winding impedances between the terminals of R and C and ground, minimizing the influence of these impedances on I_1 and I_2 [11]. The degradation of these pumps with frequency is included in the impedance errors given in Table I.

At balance the test current I for leading power factor is given by

$$I = [(d_1 V_1/R)N_{10} - (d_2 V_1 j\omega C)N_{10}] \cdot (1/N_8)(N_6/N_5) \quad (1)$$

and the apparent power is expressed in terms of the active power P and the reactive power Q by

$$\begin{aligned} VI &= P + jQ \\ &= [d_1(V^2(N_3/N_2)/R)N_{10} - j(d_2(V^2(N_3/N_2)\omega C)N_{10})] \cdot (1/N_8)(N_6/N_5) \end{aligned} \quad (2)$$

where

$$V_1 = VN_3/N_2.$$

III. ERROR ANALYSIS

The various sources of in-phase and quadrature error and their estimated uncertainties are listed in Table I.

The root-sum-square of the components which influence P and Q are given as coefficients A , B , C , and D in Table I. The associated uncertainties U_p and U_q may be expressed in terms of these coefficients and the phase angle θ between the test voltage and current:

$$\begin{aligned} U_p &\approx [A^2 \cos^2 \theta + B^2 \sin^2 \theta]^{1/2} \\ U_q &\approx [C^2 \sin^2 \theta + D^2 \cos^2 \theta]^{1/2}. \end{aligned} \quad (3)$$

Equation (3) leads to a minimum figure of 11 ppm for active power at 50/60 Hz and a maximum figure of 165 ppm for reactive power at 20 kHz. The standard deviation, S , of an actual measurement includes the random error of the wattmeter under test and is expressed (in accordance with [12]) as

$$S = [a^2 + b^2/3]^{1/2}$$

where

- a standard deviation of the mean of wattmeter readings,
- b either U_p or U_q depending on the power component.

IV. SUMMARY AND CONCLUSIONS

Design considerations and preliminary experimental results have been described for an audio-frequency power bridge which is still undergoing system-based evaluation. Principal components have been constructed, and tested, and their error limits established. Work is still in progress

to characterize the system, particularly above 1 kHz. At power frequencies, system uncertainties of less than 20 ppm are comparable with the earlier power-frequency bridge [2]. The main difference is that the earlier bridge operated with smaller reference currents, permitting the use of stable low-loss, gas-dielectric capacitors. The higher value solid-dielectric capacitors must supply the larger reference currents needed for the broad-band current comparators in the new bridge.

The use of a current comparator-based power bridge for basic realization of ac power at the conventional power frequencies of 50–60 Hz is a well established technology capable of accuracies in the 10–20 ppm range. The extension of the same technology to audio frequencies is conceptually attractive but not simple in practice. While similar principal components can be used at power as well as audio frequencies, the detailed implementation of these components is such as to restrict their highest accuracy over a relatively narrow band of frequencies. The development of a broad-band system may involve some sacrifice in accuracy, use of more sophisticated components and compensation techniques and, in extreme cases, use of duplicate components for different frequency ranges.

In the iterative process involving design, redesign, and testing of critical components, all of the above realities were encountered. It is entirely unrealistic to expect the same high accuracy over the audio-frequency range as that which can be achieved at power frequencies. For scaling voltages, specially designed binary inductive dividers had to be substituted for more conventional and commercially available decade dividers. Two current comparators and two voltage transformers, each designed to cover over a decade of frequencies, were required for the entire frequency range.

The greatest difficulty encountered was the unavailability of routine calibration capabilities for precision resistance and capacitance elements above power frequencies. As mentioned earlier, audio-frequency calibrations for impedances R and C are not readily available at the parts per million level, although the state of the art for impedance measurements is considerably better than the figures in Table I imply. Calibration techniques are being developed which make use of the phase linearity of the digital waveform generator, as well as the wide-band accuracy of the BIVD's and the current comparators. It is expected that the relatively large uncertainties presently assigned to R and C may be reduced considerably.

A source of error in all systems is the uncertainty in the ac voltage measurement. 5-ppm uncertainty in the 60-Hz voltage measurement results in a 10-ppm uncertainty in power. Above 1 kHz the TVC accuracy degrades rapidly and more basic measurement techniques using thermal converter standards are required to verify the accuracy of voltage measurements made between 1–20 kHz. Several alternate techniques are being considered which could reduce the voltage uncertainty at higher frequencies to 10 ppm.

The design, construction, and evaluation of principal

system components is nearly completed and experimental results to date indicate that the performance goals are attainable. Preliminary power comparisons between this bridge and the earlier power-frequency version were performed using a stable time-division-multiplier wattmeter [13] as a transfer standard. The agreement was within 15 ppm at 60 Hz and 50 ppm at 400 Hz.

ACKNOWLEDGMENT

The authors wish to thank R. Palm and M. Donabella for their valuable contribution in the fabrication, testing, and documentation of system components, and M. Souders for his suggestions in designing and testing current transformers.

REFERENCES

- [1] G. N. Stenbakken, "A wideband sampling wattmeter," *IEEE Trans. Power App. Syst.*, vol. PAS-103, pp. 2919-2926, Oct. 1984.
- [2] N. M. Oldham and O. Petersons, "Calibration of standard wattmeters using a capacitance bridge and a digital generator," *IEEE Trans. Instrum. Meas.*, vol. IM-34, pp. 521-524, Dec. 1985.
- [3] W. J. M. Moore and E. So, "A current-comparator-based system for calibrating active/reactive power and energy meters," *IEEE Trans. Instrum. Meas.*, vol. IM-32, pp. 147-149, Mar. 1983.
- [4] C. A. Hoer and W. L. Smith, "A 1-MHz binary inductive voltage divider with ratios of 2" to 1 or 6n dB," *IEEE Trans. Instrum. Meas.*, vol. IM-17, pp. 278-285, Dec. 1968.
- [5] N. M. Oldham, O. B. Laug, and B. C. Waltrip, "Digitally synthesized power calibration source," *IEEE Trans. Instrum. Meas.*, vol. IM-36, pp. 341-346, June 1987.
- [6] O. B. Laug, "A precision power amplifier for power/energy calibration applications," *IEEE Trans. Instrum. Meas.*, vol. IM-36, pp. 994-1000, Dec. 1987.
- [7] O. B. Laug, "A wide-band transconductance amplifier for current calibrations," *IEEE Trans. Instrum. Meas.*, vol. IM-34, pp. 639-642, Dec. 1985.
- [8] N. L. Kusters and L. G. Cox, "An automatic rms/dc comparator," *IEEE Trans. Instrum. Meas.*, vol. IM-23, pp. 322-325, Dec. 1974.
- [9] N. M. Oldham, "A 50-ppm ac reference standard which spans 1 Hz to 50 kHz," *IEEE Trans. Instrum. Meas.*, vol. IM-32, pp. 176-179, Mar. 1983.
- [10] O. Petersons and W. E. Anderson, "A wide-range high-voltage capacitance bridge with one ppm accuracy," *IEEE Trans. Instrum. Meas.*, vol. IM-24, pp. 336-344, Dec. 1975.
- [11] W. J. M. Moore and K. Ayukawa, "A current comparator bridge for power measurement," *IEEE Trans. Instrum. Meas.*, vol. IM-25, pp. 550-553, Dec. 1976.
- [12] BIPM, "Working group on the statement of uncertainties," *Metrologia*, vol. 17, no. 2, p. 73.
- [13] P. N. Miljanic and B. Stojanovic, "The development of a high precision time-division power meter," in *Proc. Conf. Prec. Electromagn. Meas.*, pp. 67-68, Aug. 1984.